LAWRENCE
LIVERMORE
NATIONAL
LABORATORY

UCRL-JRNL-207686

Chemical Origins of Permanent Set in a Peroxide Cured Filled Silicone Elastomer - Tensile and 1H NMR Analysis

S. Chinn, S. Deteresa, A. Shields, A. Sawvel, B. Balazs, R. S. Maxwell

November 4, 2004

Polymer Degradation and Stability

Chemical Origins of Permanent Set in a Peroxide Cured Filled Silicone Elastomer – Tensile and ^{1}H NMR Analysis

Sarah Chinn, Steve DeTeresa, Al Shields, April Sawvel, Bryan Balazs, Robert S.

*Maxwell**

Center for National Security Applications of Magnetic Resonance
Chemistry and Material Science Directorate
Lawrence Livermore National Laboratory
Livermore, CA 94551

Abstract:

The aging of a commercial filled siloxane polymeric composite in states of high stress and Co-60 γ-radiation exposure has been studied. DC-745 is a commercially available silicone elastomer consisting of dimethyl, methyl-phenyl, and vinyl-methyl siloxane monomers crosslinked with a peroxide vinyl specific curing agent. It is filled with ~ 30 wt.% mixture of high and low surface area silicas. This filled material is shown to be subject to permanent set if exposed to radiation while under tensile stress. Tensile modulus measurements show that the material gets marginally softer with combined radiation exposure and tensile strain as compared to material exposed to radiation without tensile strain. In addition, the segmental dynamics as measured by both uniaxial NMR relaxometry and Multiple Quantum NMR methods indicate that the material is undergoes radiatively-induced crosslinking in the absence of tensile strain and a combination of crosslinking and strain dependent increase in dynamic order parameter for the network chains. The MQ-NMR also suggests a small change in the number of polymer chains associated with the silica filler surface. Comparison of the prediction of the relative change in crosslink density from the NMR data as well as solvent swelling data and from that predicted from the Tobolsky model suggest that degradation leads to a deviation from Gaussian chain statistics and the formation of increased numbers of elastically ineffective network chains.

Keywords: Siloxanes, Radiation, Multiple Quantum NMR, Permanent Set, Unilateral NMR

***Corresponding Author**
7000 East Ave/L-231
Livermore, CA 94551
Phone: (925) 423-4991
Email: maxwell7@llnl.gov

1.0 Introduction

Filled silicon rubbers are widely used for a number of engineering, scientific, and industrial applications due in no small part to their wide applicable service temperature range, excellent non-adhesive properties, low toxicity, low chemical reactivity, and broad range of tailorable viscoelastic properties [1-3]. This tailorability is reflected in the near infinite number of industrial and laboratory formulations that have been developed with a variety of crosslink densities, filler type and content, and monomer type and concentration. Due to this versatility, these materials have been used in a wide variety of applications, from construction caulking to advanced aerospace components.

Developing life time estimates for these materials, particularly in harsh environments while under physical stress, requires detailed knowledge of the degradation pathways and the resulting effects on service properties such as component dimensions or tensile and compressive moduli. For example, elastomeric materials subject to physical stress while undergoing crosslinking reactions are known to be subject to permanent set [4, 5]. This degradation can limit component lifetime or simply have important consequences on the assessment of physical properties for lifetime assessments of field aged materials. An example of such degradation is shown in Figure 1 and illustrated the complexity of accurate determination of mechanical properties when permanent deformation results in sample shapes incompatible with traditional mechanical measurements. Thus, there is a need to apply non-standard, indirect methods to establish the effects of chemical changes to the network structure in deformed samples.

Nuclear magnetic resonance methods have shown significant ability to quantify chemical and network changes occurring during siloxane elastomer degradation [6-16].

In such materials, residual dipolar couplings between proton nuclear spins have been shown to be the result of topological constraints interfering with fast reorientations on the NMR timescale that otherwise would be expected to average homonuclear dipolar couplings to zero. The residual dipolar couplings, in fact, have been shown to be quite sensitive to dynamic and morphological changes [6-30]. The measurement of residual dipolar couplings is possible, for example, with standard relaxation time (spin-echo) methods using both standard laboratory instrumentation on excised samples of damaged components and non-destructively on intact components using portable unilateral NMR relaxometers [24].

Measurements of residual dipolar couplings via relaxation studies, however, can be complicated, due to the simultaneous effects of couplings over a wide range of length and time scales [15]. More recently, it has been reported that the characterization of the growth of multiple quantum coherences can provide additional insight into silicone network structure by increasing the selectivity of the NMR experiment to the structure and dynamics most connected to the polymer network [18-21,26-30].

In this paper, we examine the effects of radiation dose and environment on the microstructural and polymer chain mobility of DC-745U, a complex, commercial, crosslinked and filled silicone elastomer. In an effort to quantify these effects we have combined traditional mechanical property assessments with unilateral NMR relaxometry and multiple quantum-NMR measurements of changes in residual dipolar couplings to discern the nature of the chemical network changes occurring due to radiation degradation during tensile stress in DC-745U. These results have then been interpreted in the context of the Tobolsky model for the affect of crosslinking on permanent set [4].

2.0 Methods

2.1 Sample preparation and aging

Samples were cured from Dow Corning 745U silicone fluid cured with Luperox 101, Varox DBPH peroxide curing agent. DC-745U fluid is a proprietary formulation with an unknown network structure. ^{1}H and $^{29}Si\{^{1}H\}$ NMR has determined that the elastomers used in the current study contained ~ 98.5% dimethyl siloxane monomers, ~ 1.5% methyl-phenyl siloxane monomers, and a small amount of vinyl siloxane monomers that are converted to short chain (N=4) alkyl crosslinking sites. The final elastomer also contains a ~30 wt.% mixture of quartz and high surface area silica fillers and small amounts of $CaCO_3$ (left over from the curing agent) for thixotropic thickening. The filled, crosslinked copolymers were characterized by a crystallization temperature @ -45 ºC and a glass transition temperature @ -120 ºC by Differential Scanning Calorimetry. Solvent swelling experiments have quantified the crosslink density, $\nu_{polymer}$, for the polymer network as 0.018 (crosslinks/monomer; $\nu_{polymer} = MW_{monomer}$/mol.weight between crosslinks)[11, 31,32].

Tensile strain was applied for a defined time for the non-control samples using the sets shown in Figure 2B. Ends of elastomer test samples were pinched between steel plates and the strain was applied by stretching the elastomer samples to the strain λ_1 = L(aging)/L(0) using preset pins. Here L(aging) and L(0) are the sample lengths in the strained and initial unstrained state. The entire tensile set was placed within the stainless steel irradiation vessel (Figure 2A). The vessel was then evacuated through an attached valve and lowered into the irradiation chamber for the specified time. The irradiation pit

contained a Co-60 source (1.2 MeV). The samples were irradiated at 5 kGray/hr for sufficient time to expose the samples to cumulative doses of 5 kGray to 250 kGray.

The length of the tensile samples irradiated under tensile strain, L(recovered), was measured after disassembly of the aging apparatus and after allowing the samples to relax for a period of 24 hours. No additional relaxation was observed for relaxation times up to 72 hours. The permanent set was then calculated according to equation {1}.

$$P_s = (\lambda_s - 1)/(\lambda_1 - 1) \qquad \{1\}$$

where λ_s = L(recovered)/L(0).

2.2 NMR methods

Static, uniaxial NMR relaxometry experiments were performed using Spin-echo decay curves obtained via a CPMG pulse sequence (Figure 3A) on an NMR Mobile Universal Surface Explorer (MOUSE) from Bruker Optics operating at 17 MHz. The experimental parameters were set as follows: echo time of 0.25 ms with 1500 echoes times per experiment and 512 scans signal averaged per echo time. The pulse attenuation, receiver gain, and recycle delay were set to 6 dB, 103 dB, and 1 s, respectively. Decay curves were processed with the Contin application from Bruker Optics, which uses an inverse Laplace transform to yield the distribution of T_2 relaxation times [24].

Multiple quantum NMR experiments were performed using the refocused multiple quantum excitation and reconversion pulse sequence shown in Figure 3B. Experiments were performed at 400.13 MHz on a Bruker Avance 400 spectrometer using a Bruker TBI (HCX) 5mm probe. In all cases, small (0.1 cm x 0.1 cm x 0.1cm) squares of

elastomer were cut from a larger piece and set in the portion of a 5 mm NMR tube that would be within the coil volume of the probe. The phases of the reconversion sequence were cycled in 90º steps with phase inversion on the observe pulse for coherence selections (the pulse sequence excites all even-multiple quantum coherences). CYCLOPS was then added to yield sixteen step phase cycle [33]. As described in 33. Saalwachter, the pulse sequence yields the total sum of the even-multiple quantum coherences, dominated by the double quantum coherences, S_{mq} [26,27]. Pulse lengths of 6.1 μs were used with delay Δ_1 and Δ_2 equal to 4.83 μs and 6.16 μs respectively. Repeat experiments with longer delay times indicated that for these delays, no artifacts due to high duty cycle were observed.

The spectral intensities from the MQ pulse sequence, $S_{mq}(t)$, were then normalized with the use of a reference spectrum obtained by removing the alternating phases on the observe pulse, S_{ref}. The normalized multiple quantum integral was obtained by calculating for each excitation time, t,

$$I_{mq}(t) = S_{mq}(t)/(S_{mq}(t)+S_{ref}(t)) \qquad \{2\}$$

In the case of spins characterized by a dominant residual dipolar coupling, the multiple quantum growth curve is then described by

$$I_{mq}(t) = A*(1-\exp(-B\langle\Omega_d\rangle^2)\, t^2) \qquad \{3\}$$

In cases where spins can be described by more than one residual dipolar coupling, as in the case of bimodal or phase separated network structures, the multiple quantum growth curves can be described by a summation of growth curves

$$I_{mq}(t) = \Sigma\, A_i*P_i*(1- \exp(-B_i \langle\Omega_d\rangle_i^2)\, t^2) \qquad \{4\}$$

Where P_i is the relative mole fraction of spins with $<\Omega_d>_i$ and B_i are pulse sequence and monomer specific constants – in the case of methyl groups in PDMS based polymers A_i = 0.5 and B_i = 31.91 [26,27].

2.4 Mechanical assessments

Tensile tests were performed on virgin and irradiated specimens to determine initial modulus and stress-strain behavior up to 20% elongation. All testing was performed with an electromechanical test system (MTS Synergie 1,000 lb) equipped with pneumatic grips and a 50N load cell. The change in width of specimens was measured during tensile testing using a laser micrometer (Keyence LS-5041). This measurement was used to determine the lateral stretch ratio, λ_2. The micrometer was mounted on a movable frame to allow the specimen width to be measured at a fixed location along the specimen length during the test. Initial lateral dimensions of the tensile specimens were determined using a comparator (Nikon Profile Projector V-12) to measure width and a height gage (Heidenhain MT12) to measure thickness. Specimens were tested using an initial gage length of 1.25 in. and a displacement rate of 0.2 in./min.

Data for tensile response are reported in terms of the Cauchy stress and axial stretch ratio, λ_1. Although the stretch ratio can be calculated from the specimen elongation given by the measured displacement of the test system crosshead, small amounts of slippage in the grips sometimes introduced error in this calculation. This problem was avoided by calculating the axial stretch ratio from the change in width of the specimen, using the assumption that the elastomer was incompressible. For an incompressible material, the three orthogonal stretch ratios are related by:

$$\lambda_1\lambda_2\lambda_3 = 1 \qquad \{5\}$$

where λ_2 and λ_3 are the lateral stretch ratios. For uniaxial extension, $\lambda_2 = \lambda_3$. Therefore the axial stretch ratio can be determined from the lateral stretch ratio using:

$$\lambda_1 = \frac{1}{\lambda_2^2} \qquad \{6\}$$

3.0 Results and Discussion

Non-recoverable tensile set, λ_s, as a function of cumulative dose and aging strain, λ_1, are shown in Figure 4A. In all cases where λ_1 was greater than 1.0, permanent set was observed in these materials. The relaxed length was observed to increase with dose and λ_1. When normalized according to equation {1}, and shown in Figure 4B, the λ_1 dependence disappeared within experimental error although the increase in P_s with dose remained and reached a maximum of 0.40 at 170 kGray. Previous studies of the effect of radiation in vacuum in the absence of physical stress in both these materials and similar filled silicones has shown that the degradation is dominated by crosslinking reactions [see below and ref 7, 8, 10-14]. These observations are in qualitative agreement with previous experimental and theoretical studies of the effects of crosslinking while under physical stress [4, 5].

Tensile modulus as a function of dose and λ_1 are shown in Figure 5 and indicate that irradiation to 170 kGray results in a dramatic hardening of the polymer composites upon exposure to radiation compared to the pristine material. This is presumably due to degradation dominated by radiative crosslinking reactions. For samples irradiated to 170 kGray under tensile strain, increased strain during irradiation produced samples that were characterized by moderate softening compared to the sample irradiated without tensile strain.

The results of static unilateral relaxometry as measured by the NMR MOUSE are shown in Figure 6 for the samples irradiated without tensile stress (top) and for those irradiated with tensile stress (Bottom). In elastomeric materials, the residual dipolar couplings observable via relaxation studies have been shown to be the result of topological constraints interfering with fast reorientations on the NMR timescale that otherwise would be expected to average homonuclear dipolar couplings to zero [6-30]. These changes can be observed through detailed study of samples in standard high field laboratory spectrometers or in new portable, uniaxial NMR relaxometers (i.e. the NMR MOUSE). The data are presented in histogram format from an inverse Lapace transform of the spin-echo decay curves, as described in [24]. All samples showed a similar width in the distribution of T_2's observed, while the average T_2 observed is clearly dose and λ_1 dependent with a decrease in T_2 with increased dose and λ_1. The mean relaxation rate, $1/T_2$, is plotted as a function of dose and λ_1 in Figure 7 and listed in Table 1. The dominant change to $1/T_2$ is due to the radiation induced crosslinking as observed from the differences in the pristine sample and the sample irradiated without tensile stain shown in the top of Figure 6. For samples irradiated to 170 kGray under increasing λ_1, a small but steady increase in $1/T_2$ was observed suggesting a small λ_1 dependent increase in crosslink density or an increase in the dynamic order parameter, S_n:

$$S_n = \langle\Omega_d\rangle/\langle\Omega_d\rangle_{static} = \tfrac{1}{2}\langle\cos^2\theta(t)-1\rangle \sim T_{2static}/T_2 \qquad \{7\}$$

Where $T_{2static}$ and $\langle\Omega_d\rangle_{static}$ are the transverse relaxation time and the dipolar coupling between proton spins in the absence of motion and $\theta(t)$ describes the time dependent angle between the local chain axis and a director. For crosslinked materials, the director is vector that connects two crosslinks [19], as shown in the inset to Figure 11.

The MQ-NMR growth curves for the pristine and 170 kGray samples with λ_1 = 1.0, 1.4, 1.6 and 1.9 samples are shown in Figure 8A. The measurement of residual dipolar couplings from relaxation time measurements alone can be complicated due to the simultaneous effects of couplings over a wide range of length and time scales [15, 26]. It has been reported that the characterization of the growth of multiple quantum coherences can provide model free insight into silicone network structure by increasing the selectivity of the NMR experiment to the structure and dynamics most connected to the polymer network [18-21, 26-30]. As can been seen, the growth curve for the pristine sample is significantly slower than the samples irradiated with or without tensile strain. Since an increase in the rate of MQ coherence growth is characteristic of an increase in residual dipolar couplings and a reduction in segmental mobility (and thus an increase in crosslink density or dynamic order parameter), this observation is consistent with the data obtained from NMR unilateral relaxometry above, that exposure to ionizing γ-radiation in nitrogen is dominated by radiative crosslinking reactions.

As mentioned above, more quantitative analysis on the network structure can be obtained by comparison of the experimental data to equations {2-4}. The MQ-growth curve for the sample irradiated to 250 kGray cumulative exposure is shown in Figure 8B along with examples of growth curves based on equations {2-4} for single average values of the residual dipolar coupling and dual populations of residual dipolar couplings consistent with dual morphology network structure. None of the experimental curves obtained in this study could be fit to a growth curve with a single $<\Omega_d>$. As a result, fits were performed using two average values of the residual dipolar coupling, $<\Omega_d>_{low}$ ~ 310 Hz and $<\Omega_d>_{high}$ ~ 800 Hz. We have previously assigned these polymer domains as

network polymer chains far from the filler surfaces and network chains near the filler surface. It is expected that polymer chains confined to or near the filler surface are described by slower segmental dynamics and thus higher residual dipolar couplings [12,14]. This expectation has been born out in DSC, dielectric relaxation, and NMR studies of polymers confined at surfaces and in restricted volumes [28, 33-38].

For the samples exposed to γ-radiation while under tensile strain, only small differences are observable in the growth curves for different λ_1. Results of the fits to equation {4} are shown in Figure 9 and listed in Table 1. The segmental dynamics of the network polymer chains were found to be described by $<\Omega_d>_{low}$ of about 350 Hz. The polymer chains associated with the filler surfaces were characterized by $<\Omega_d>_{high}$ near 820 Hz. With an increase in λ_1 from 1.4 to 1.9, $<\Omega_d>_{low}$ increased by 14 %, $<\Omega_d>_{high}$ increased by ~ 4% and the amount of polymer associated with the filler surface, X_{high}, decreased by ~ 5.4%. The smaller relative increase in the segmental dynamics measured by the MQ method compared to the NMR MOUSE method is not unexpected. Detailed analysis of relaxation based approaches and MQ-based approaches, in fact, have indicated that relaxation time based methods tend to overestimate the residual dipolar couplings [15, 26].

Results of solvent swelling in toluene for the pristine samples and samples aged under tensile strain are listed in Table 1 and indicate radiation exposure to a cumulative dose of 170 kGray alone lead to an increase in crosslink density of ~ 140%. Samples irradiated under tensile strain did not show a difference in crosslink density, ν_{poly}, as a function of λ_1 within experimental error. The lack of any change in ν_{poly} with λ_1 suggests that the changes in the NMR observables, $<\Omega_d>_{low}$, $<\Omega_d>_{high}$, and $1/T_2$, are due not to a

decrease in segmental dynamics brought about by an increased crosslink density, but rather by an increase in the dynamic order parameter, S_n. The fundamental assumption of the Tobolsky Model for permanent set is that crosslinks formed under strain are formed in a state of zero stress – i.e. formed while the polymer network is stretched and aligned along the tensile strain axis [4]. This implies that the polymer chains formed between newly formed crosslinks were formed in an elongated state, with director n, compared to the original network junctions, as shown in Figure 11. As λ_1 was increased, the degree of elongation of the new network chains increased. The consequence for the NMR measurements is a relative decrease in the amplitude of the motions about this director, and an increase in the dynamic order parameter described in equation {7}.

Previous studies on silicone based materials have established the general empirical correlation between crosslink density and residual couplings, either from MQ-NMR or from relaxation time studies [6-15]. In general, $1/T_2$ or $<\Omega_d>$ have been found to be linear with respect to crosslink density over limited ranges. As such, we have calculated the relative increase in crosslink density for samples irradiated under stress from the relative change in NMR observable and the results are shown in Figure 10. In addition, one can predict the change in crosslink density while irradiated under stress from the mathematical framework developed by Tobolsky. In this case, using the assumptions that a) the network can be described as near Gaussian and b) no net change occurs in the number of elastically ineffective chains, the permanent set is a function of the ratio of the crosslink density at the start of the experiment to the crosslink density at the end of the experiment [4,5]:

$$P_s = \frac{\lambda_1 \left[\frac{\nu_1/\nu_0 - 1/\lambda_1}{\nu_1/\nu_0 - \lambda_1^2} \right]^{1/3} - 1}{\lambda_1 - 1} \qquad \{8\}$$

The ratio of the crosslink density at the cumulative doses shown compared to the crosslink densities derived from both NMR and solvent swelling results on samples irradiated in unstressed states are shown in Figure 10 as well. As can be seen in Figure 10, the Tobolsky model reasonably predicts the relative change in network structure at low doses, but overestimates the crosslink density at high doses. This discrepancy can be rationalized by reference to the assumptions used in deriving equation {7}, i.e. Gaussian chain statistics and a constant amount of elastically ineffective chains. It has been shown that at high doses for similar materials a deviation from Gaussian chain statistics does indeed occur [12,13]. In addition, it is highly likely that with increasing dose an increasing number of elastically ineffective chains are being created by the formation of crosslinks that close off loops, as illustrated in Figure 11.

4.0 Conclusions

We have shown that a combined use of traditional polymer assessment methods with advanced NMR relaxometry methods can provide improved insight into the degradation of silicone elastomers that leads to permanent set. An illustration of the degradation mechanisms are shown in Figure 11. Our results on the commercial, silica filled silicone elastomer, DC-745U, studied here have quantified the amount of tensile set that occurs in these materials when irradiated under strain. Unilateral NMR relaxometry using the NMR MOUSE and multiple quantum NMR spectroscopy using high field instrumentation have quantified the changes in segmental dynamics occurring in these

materials. NMR relaxation times indicate an overall reduction in the segmental mobility in samples irradiated with and without tensile strain. The MQ NMR results indicate that the majority of the damage that is occurring in these materials with the addition of tensile strain is a crosslinking of the polymer network (decrease of ~15% in segmental dynamics) rather than a change in the filler-polymer interaction (decrease of ~ 5% in amount of surface interacting polymer) that is seen with radiation exposure alone. Tensile testing of the damaged and set materials, in contrast indicates that the materials are softening. This would imply an effect of chain scissioning or a reduction in the filler-polymer interactions. Though radiation exposure does lead to competing rates of chain scissioning and crosslinking in all polymers, the radiation induced degradation in silicone polymers is well known to be dominated by crosslinking reactions [7, 8, 11-14]. A reduction in the filler-polymer interaction has been observed in the MQ NMR measurements and given the small decrease in tensile stiffness in these materials it is likely that it is this reduction that is responsible for the softening affect. Comparison to the Tobolsky model for the effect of network changes on permanent set in elastomers suggests that with damage the polymer network rearranges it self to vary statistically from a Gaussian distribution and forms increasing numbers of elastically ineffective chains. Both of these effects may also contribute to the softening observed in the tensile testing experiments.

5.0 Acknowledgments

This work was performed under the auspices of the U.S. Department of Energy by the University of California, Lawrence Livermore National Laboratory under contract

#W-7405-Eng-48. The authors would like to thank Jeff DeBisschop for performing the irradiations and Mel Bishop for miscellaneous glass fabrication work.

6.0 References

1. Zeigher J M, Fearon F W G, Silicon Based Polymer Science: A Comprehensive Resource. Advances in Chemistry 224, Washington, DC: ACS Press; 1990.
2. Clarson S J, Semlyen J A. Siloxane Polymers New Jersey: Prentice Hall; 1993
3. Brook M A. Silicon in Organic, Organometallic, and Polymer Chemistry. New York: Wiley; 2000.
4. Rottach D R, Curro J G, Grest G S, Thompson A P. Effect of Strain History on Stress and Permanent Set in Cross-linking Networks: A Molecular Dyanamics Study, Macromolecules 2004; 34:5468-5473
5. Andrews R D, Tobolsky A V, Hanson E E, The Theory of Permanent Set at Elevated Temperatures in Natural and Synthetic Rubber. J. Appl. Phys 1946; 17:352-361.
6. Cohen-Addad J P, Dupeyre R. Strongly entangled polymer chains in a melt. Description of n.m.r. Polydimethylsiloxane. Int J Radiat Phys Chem 1976; 8(5): 555-62.
7. Charlesby A, Folland R. The Use of Pulsed NMR to Follow Radiation Effects in Long Chain Polymers. Radiat Phys Chem 1983; 15: 393-402.
8. Folland R, Charlesby A. Pulsed NMR studies of crosslinking and entanglements in high molecular weight linear polydimethylsiloxanes. Radiat Phys Chem 1977; 10: 61-68.
9. Litvinov V M, Zhdanov A A. Molecular motions in filled polydimethylsiloxanes. Polymer Science USSR 1987; **29**: 1133-1139.
10. Folland R, Steven J H, Charlesby A. Proton spin relaxation in liquid polydimethylsiloxane: molecular motion and network formation. J Poly Sci 1978; **16**, 1041-1057.
11. Chien A, Maxwell R S, Chambers D, Balazs B, LeMay J, Characterization of radiation-induced aging in silica-reinforced polysiloxane composites. J Rad Phys Chem 2000; 59(5-6): 493-500.
12. Maxwell R S, Balazs B, Residual dipolar coupling for the assessment of crosslink density changes in γ-irradiated silica-PDMS composite materials. J Chem Phys 2002; 116: 10492-10502.
13. Maxwell R S, Cohenour R, Sung W, Solyom D, Patel M, The effects of γ-radiation on the thermal, mechanical, and segmental dynamics of a silica filled, room temperature vulcanized polysiloxane rubber. Poly Deg Stab 2003; 80(3):443-450.
14. Chinn S, Maxwell R S, Cohenour R, Solyom D. Radiation induced network changes in a peroxide cured silicone elastomer as investigated by Multiple Quantum 1H NMR, Polymer, 2004; submitted.
15. Cohen-Addad J P. NMR and Fractal Properties of Polymer Liquids and Gels, Prog NMR Spect 1993; 25:1-316.
16. W. Gronski W, Hoffmann U, Simon G, Wutzler A, Straube E. Structure and Density of Crosslinks in Natural Rubber Vulcanates. A Combined Analysis by NMR Spectroscopy, Mechanical Measurements, and Rubber-Elastic Theory. Rubber Chem. Tech *1992;* 65 63-77.
17. Grinberg F, Garbarczyk M, Kuhn W. Influence of the cross-link density and the filler content on segment dynamics in dry and swollen natural rubber studied by the NMR dipolar-correlation effect. Journal of Chemical Physics. 1999; 111(24):11222-11231.
18. M. Schneider M, Gasper L, Demco D E, Blumich B. Residual dipolar couplings by H-1 dipolar-encoded longitudinal magnetization, double- and triple-quantum nuclear magnetic resonance in cross-linked elastomers. J Chem Phys 1999; **111,** 402-415.
19. Dollase, T, Graf R, Heuer A, Spiess H W. Local order and chain dynamics in molten polymer blocks revealed by proton double-quantum NMR. Macromolecules, 2001*;* **34,** 298-309.
20. Graf R, Heuer A, Spiess H W. Chain-Order Effects In Polymer Melts Probed By H-1 Double-Quantum NMR Spectroscopy. Phys. Rev. Lett., 1998*;* **80** 5738-5741.
21. Graf R, Demco D E, Hafner S, Spiess H W, Selective Residual Dipolar Couplings In Cross-Linked Elastomers By H-1 Double-Quantum NMR Spectroscopy. Solid State NMR, 1998; **12:** 139-152.
22. Callaghan P T, Samulski E T. Molecular ordering and the direct measurement of weak proton-proton dipolar interactions in a rubber network. Macromolecules, 1997; 30(1): 113-122.
23. Callaghan PT. Samulski ET. Molecular weight dependence of nuclear spin correlations in PDMS networks. Macromolecules. 2000; 33(10):3795-3802.
24. Eidmann G, Savelsberg R, Blumler P, Blumich B. The NMR MOUSE, a mobile universal surface explorer. J Mag Res A, 1996; 122:104-109.
25. Grinberg F, Kimmich R, Moller M, Molenberg A. Order Fluctuations In The Mesophase Of Polydiethylsiloxane As Studied By The Dipolar-Correlation Effect On The Stimulated Echo. J Chem Phys 1996; **105**: 9657-9665.

26. Saalwachter K, Ziegler P, Spyckerelle O, Haidar H, Vidal A, Sommer J-U. H-1 multiple-quantum nuclear magnetic resonance investigations of molecular order distributions in poly(dimethylsiloxane) networks: Evidence for a linear mixing law in bimodal systems. J CheM Phys 2003; 119 (6): 3468-3482.
27. Saalwachter K. H-1 multiple-quantum nuclear magnetic resonance investigations of molecular order in polymer networks. II. Intensity decay and restricted slow dynamics. J Chem Phys 2004; 120(1):454-464.
28. Fechete R, Demco D E, Blumich B, Segmental anisotropy in strained elastomers by H-1 NMR of multipolar spin states. Macromolecules 2002 ; 35: 6083-6085.
29. Wang M, Bertmer M, Demco D E, Blumich B, Litvinov V M, Barthel H. Indication of heterogeneity in chain-segment order of a PDMS layer grafted onto a silica surface by H-1 multiple-quantum NMR. Macromolecules 2003; 36: 4411-4413.
30. Fechete R, Demco D E, Blumich B, Enhanced sensitivity to residual dipolar couplings of elastomers by higher-order multiple-quantum NMR. J Mag Res 2004; 169(1):19-26.
31. Flory P J. Principles of Polymer Chemistry, Cornell University Press, Ithaca, New York (1953).
32. French D. Crosslink density and solvent swelling of filled and unfilled stocks. J. Appl. Poly. Sci., 1980; 25: 665-682.
33. Ernst R R, Bodenhausen G, Wokaun A., Principles of Nuclear Magnetic Resonance in One and Two Dimensions, New York; Oxford University Press; 1987.
34. Lorthioir C, Alegria A, Colmenero J, Deloche B, Heterogeneity of the Segmental Dyanamics of Poly(dimethylsiloxane) in a Diblock Lamellar Mesophase: Dielectric Relaxation Investigations. Macromol. 2004; 37: 7808-7817.
35. Hartmann L, Kremer F, Pouret P, Leger L, Molecular dyanamics in grafted layers of poly(dimethylsiloxane) J. Chem. Phys. 2003; 118: 6052-6058
36. Kremer F, Hartmann L, Serghei A, Pouret P, Leger L, Molecular dynamics in thin grafted and spin-coated polymer layers. Eur. Phys. J E 2003; 12: 139-142
37. Lorthioir C, Auroy P, Deloche B, Gallot Y, Chain segment ordering in lamellar sublayers of block copolymers: A NMR study. Eur Phys. J. E. 2002; 7: 261-266
38. Schonhals A, Goering H, Schick C H, Frick B, Zorn R, Glassy dynamics of polymers confined to nanoporous lasses revealed by relaxational and scattering experiments. Eur. Phys. J. E 2003; 12: 173-178

Table 1. Results of experimental parameters for samples studied.

	Tensile Modulus (PSI)	$\%\Delta\nu_{polymer}$ (+/- 7%)	$1/T_2$ (ms^{-1})	X_{long}	$\langle\Omega_d\rangle^2_{long}$ (Hz)	$\langle\Omega_d\rangle^2_{short}$ (Hz)
Pristine	484	0	0.011	0.15	690	280
170 kGray, λ_1=1.0	747	140	0.012	0.37	820	360
170 kGray, λ_1=1.2	705	145	0.012	0.37	815	350
170 kGray, λ_1=1.4	574	138	0.013	0.37	820	360
170 kGray, λ_1=1.6	562	156	0.014	0.37	820	380
170 kGray, λ_1=1.9	536	136	0.015	0.35	850	410

7.0 List of Figure Captions

Figure 1. Photo of permanent set of elastomer dogbones irradiated under vacuum while under complex stress.

Figure 2. Photograph of irradiation chamber and sample fixture.

Figure 3. Pulse sequences used in this study, A) CPMG echo train; B) multiple quantum excitation, reconversion, and observe sequence. Details of pulse phases and delays are discussed in the text.

Figure 4. (A) Permanent set, Ps, as a function of dose and strain, λ_i; (B) permanent set normalized to strain, $\lambda_i(0)$.

Figure 5. Tensile stress as a function of tensile strain for samples irradiated to 170 kGray with varying tensile strains during irradiation, λ_1.

Figure 6. T_2 histograms obtained from NMR MOUSE; (A) samples irradiated without tensile strain; (B) samples irradiated with tensile strain.

Figure 7 (A) Average relaxation rate, $1/T_2$, versus (A) dose and (B) λ_1 for samples irradiated under tensile strain.

Figure 8. Representative plot of I_{MQ} as a function of MQ mixing time for (A) increasing values of the residual dipolar coupling, $<\Omega_d>$ = 340, 850, and 600 Hz (the first two are scaled to 0.5 of their expected intensity); (B) Dual morphology model, described by equation {4} with equal populations of sites with $<\Omega_d>_1$ = 350 and $<\Omega_d>_2$ = 850 Hz.

Figure 9. Results of 4 parameter fits to equation {X} of $I_{MQ}(t)$ curves shown in Figure 8A as a function of cumulative dose: changes in residual dipolar couplings, $<\Omega_d>_1$ and $<\Omega_d>_2$; Changes in mole fraction, X_1 and X_2, were small and are listed in Table 1.

Figure 10. Relative changes in crosslink density (CLD) due to exposure to g-radiation as predicted from equation {8} and observed experimentally by NMR and solvent swelling.

Figure 11. Representative illustration of multilevel degradation processes contributing to the overall degradation and the origins of permanent set in occur in the irradiated PDMS elastomers studies. Large circle represents filler particle, curves represent polymer chains, crosslinks are designated by small dark circles, and the inset indicates the definition of the angle between the director n and the local chain segment that defines the dynamic order parameter, S_n.

Figure 1.

Figure 2.

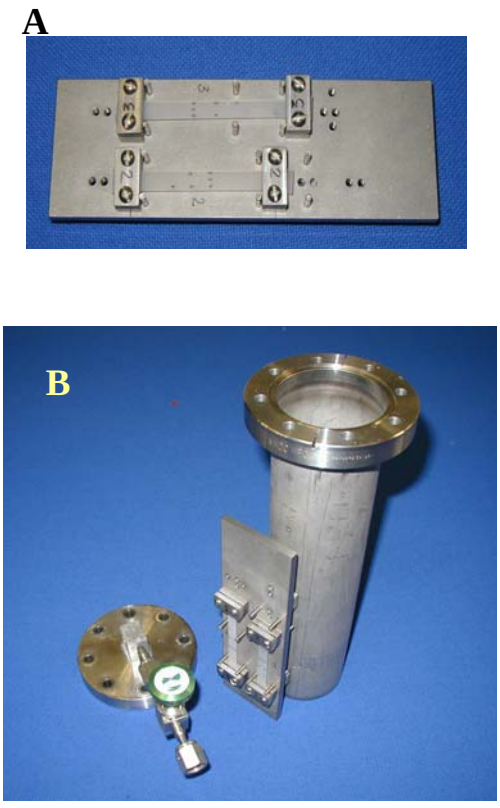

Figure 3.

A.

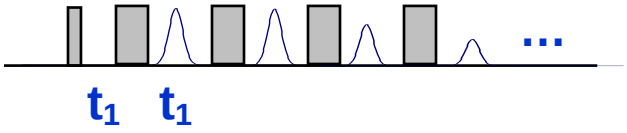
...
t1 t1

B.

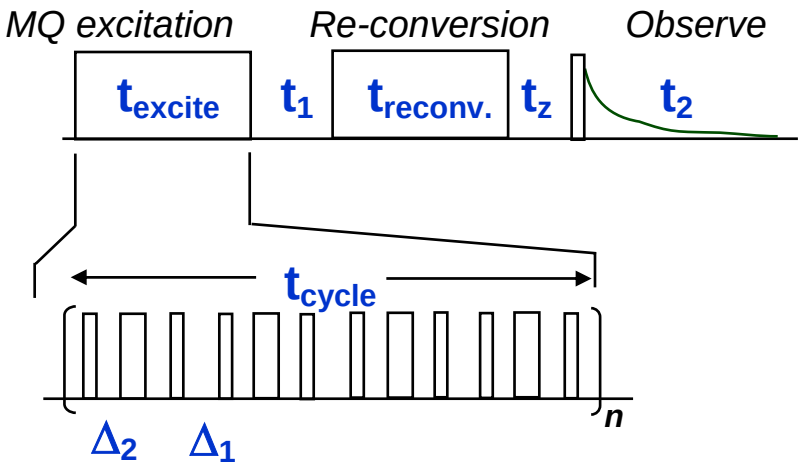
MQ excitation
Re-conversion
Observe
texcite
t1
treconv.
tz
t2
tcycle
n
Δ2
Δ1

Figure 4.

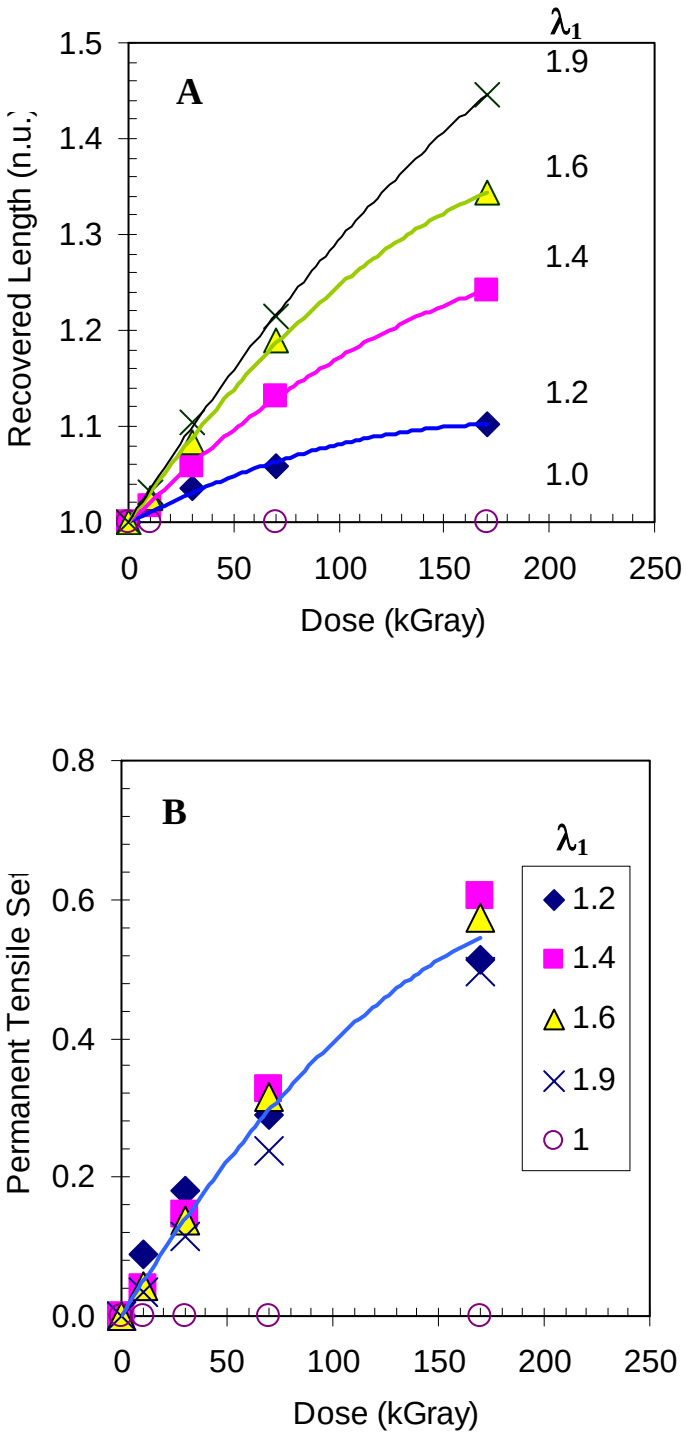
A
B
λ1
1.9
1.6
1.4
1.2
1.0
Recovered Length (n.u.)
Permanent Tensile Set
Dose (kGray)
0
50
100
150
200
250
1.5
1.4
1.3
1.2
1.1
1.0
0.8
0.6
0.4
0.2
0.0
1

Figure 5.

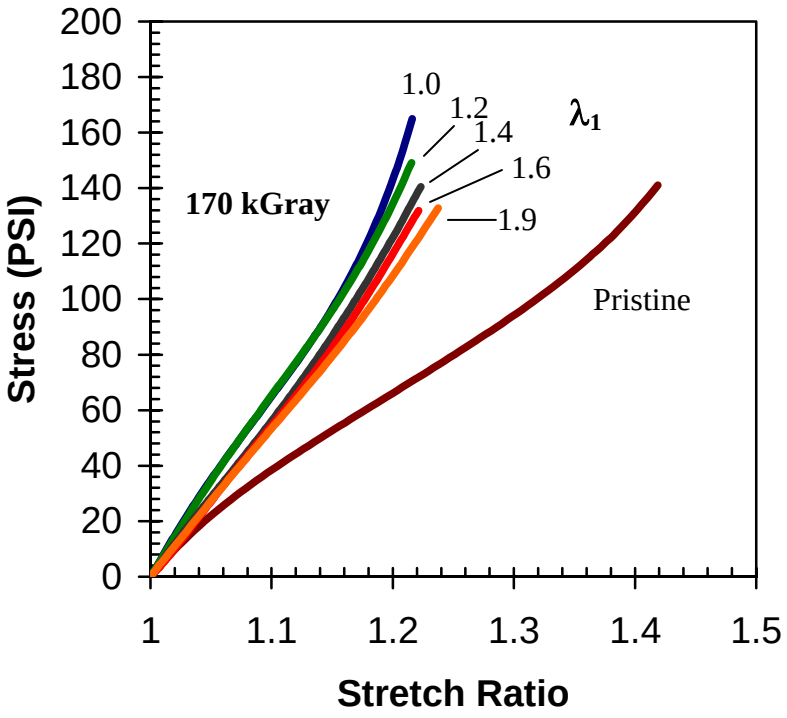
200
180
160
140
120
100
80
60
40
20
0
Stress (PSI)
1
1.1
1.2
1.3
1.4
1.5
Stretch Ratio
170 kGray
1.0
1.2
1.4
1.6
1.9
λ1
Pristine

Figure 6.

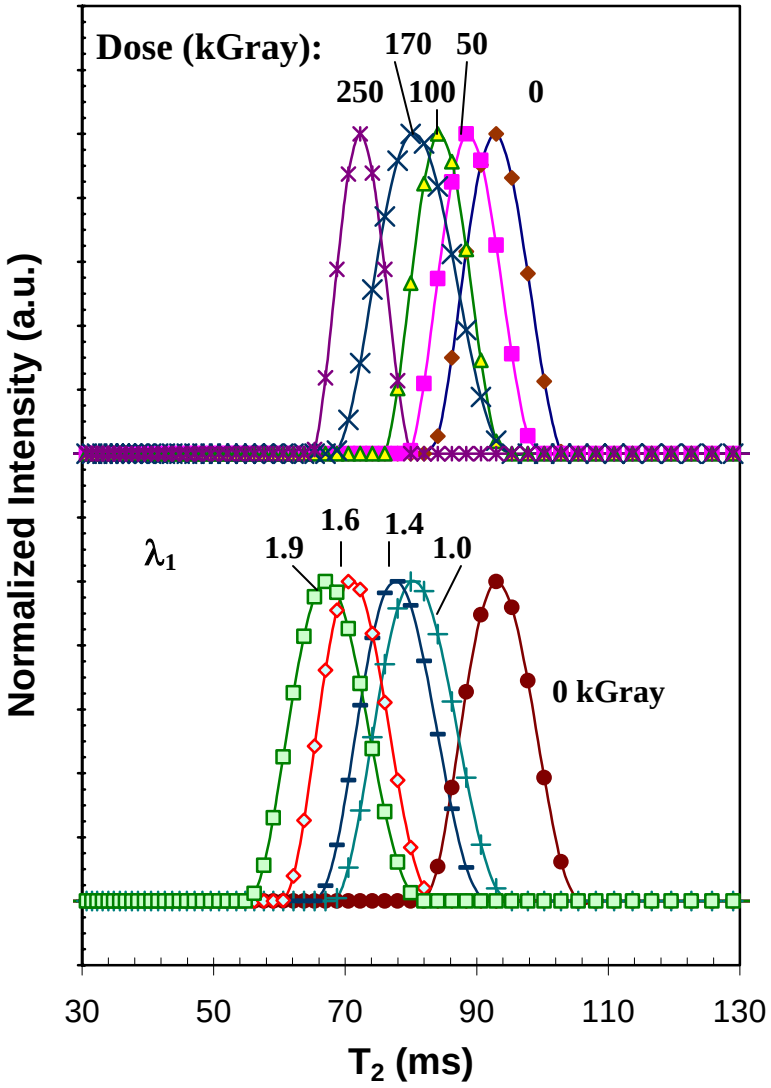
Dose (kGray):
170
50
250
100
0
λ1
1.9
1.6
1.4
1.0
0 kGray
Normalized Intensity (a.u.)
30
50
70
90
110
130
T2 (ms)

Figure 7

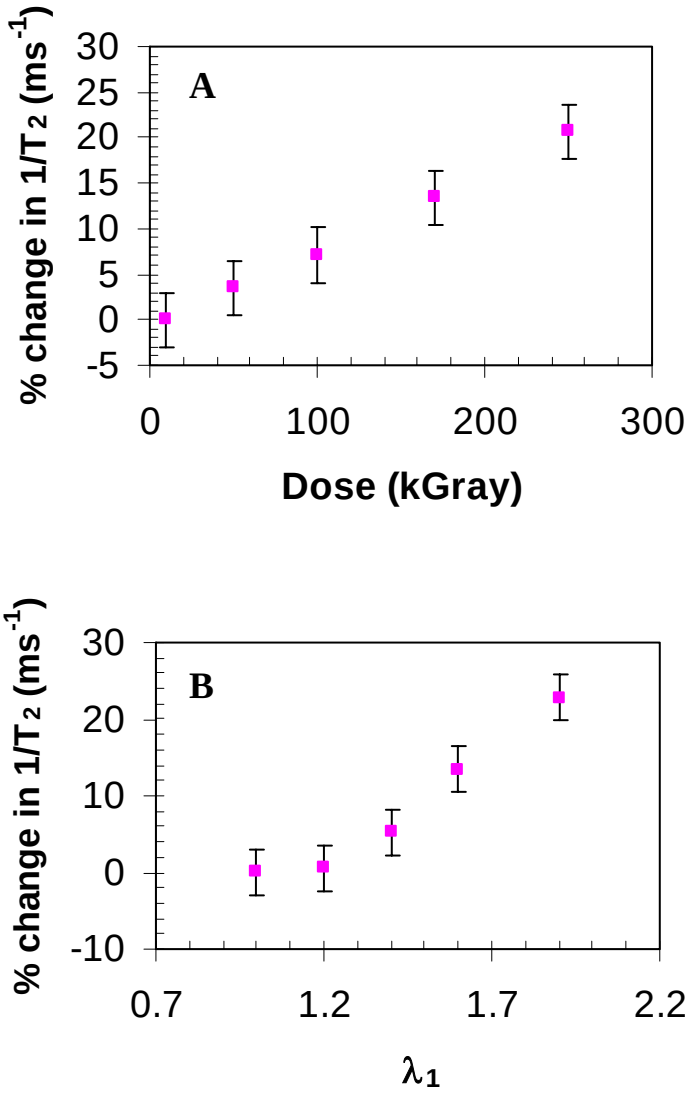
A
% change in 1/T2 (ms-1)
30
25
20
15
10
5
0
-5
0
100
200
300
Dose (kGray)
B
% change in 1/T2 (ms-1)
30
20
10
0
-10
0.7
1.2
1.7
2.2
λ1

Figure 8.

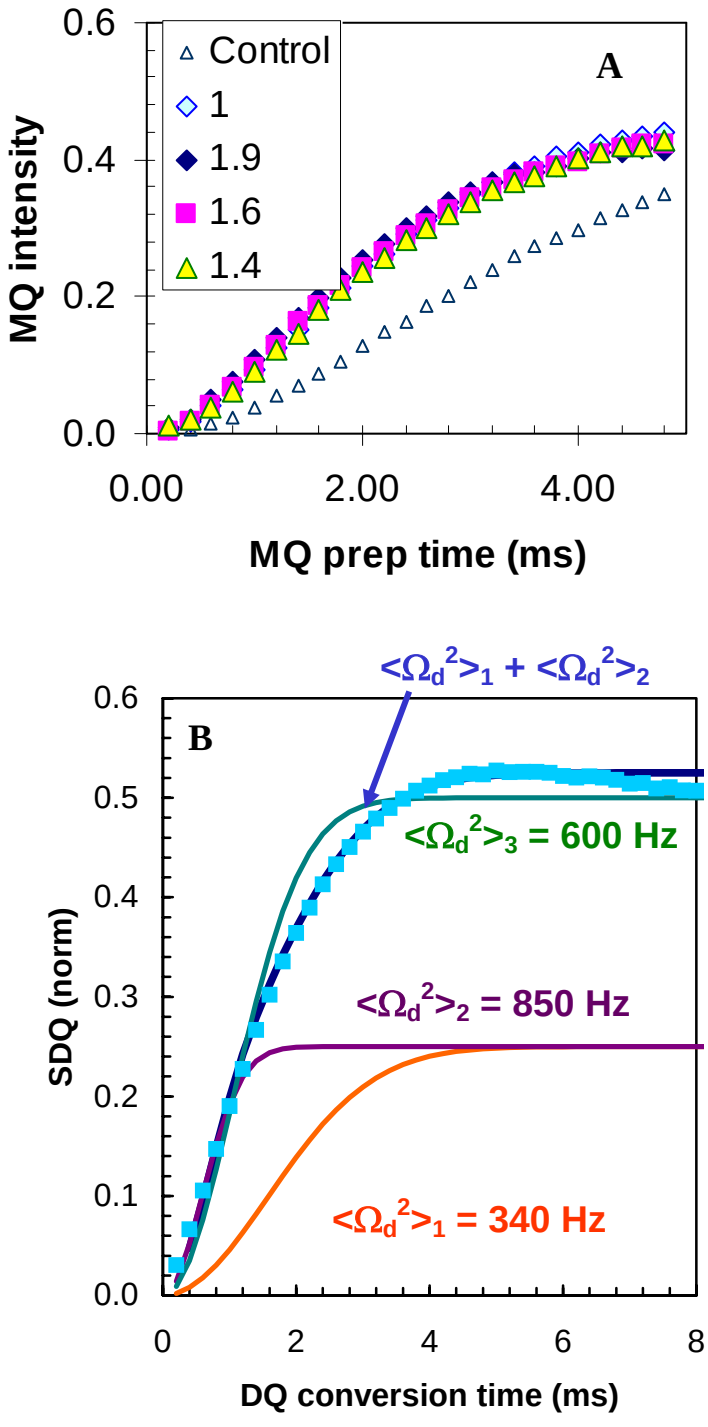
A
Control
1
1.9
1.6
1.4
MQ intensity
MQ prep time (ms)
0.0
0.2
0.4
0.6
0.00
2.00
4.00
B
$\langle\Omega_d^2\rangle_1 + \langle\Omega_d^2\rangle_2$
$\langle\Omega_d^2\rangle_3$ = 600 Hz
$\langle\Omega_d^2\rangle_2$ = 850 Hz
$\langle\Omega_d^2\rangle_1$ = 340 Hz
SDQ (norm)
DQ conversion time (ms)
0.0
0.1
0.2
0.3
0.4
0.5
0.6
0
2
4
6
8

Figure 9.

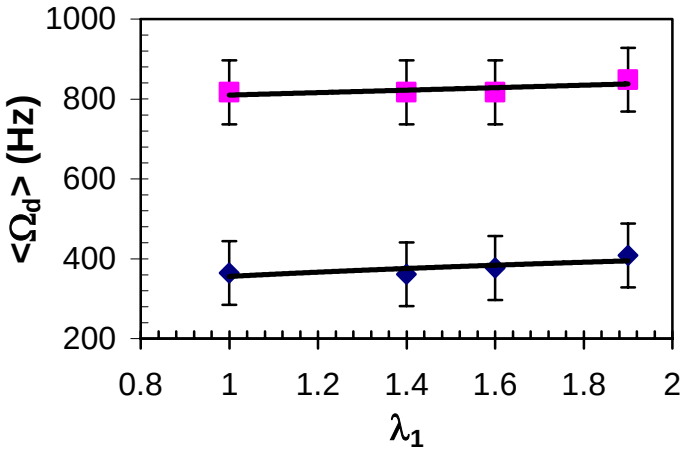

Figure 10

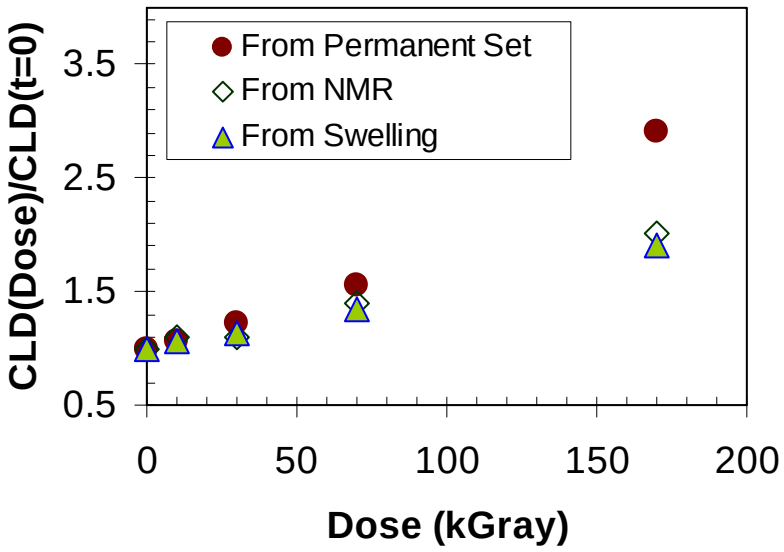
From Permanent Set
From NMR
From Swelling
CLD(Dose)/CLD(t=0)
3.5
2.5
1.5
0.5
0
50
100
150
200
Dose (kGray)

Figure 11.

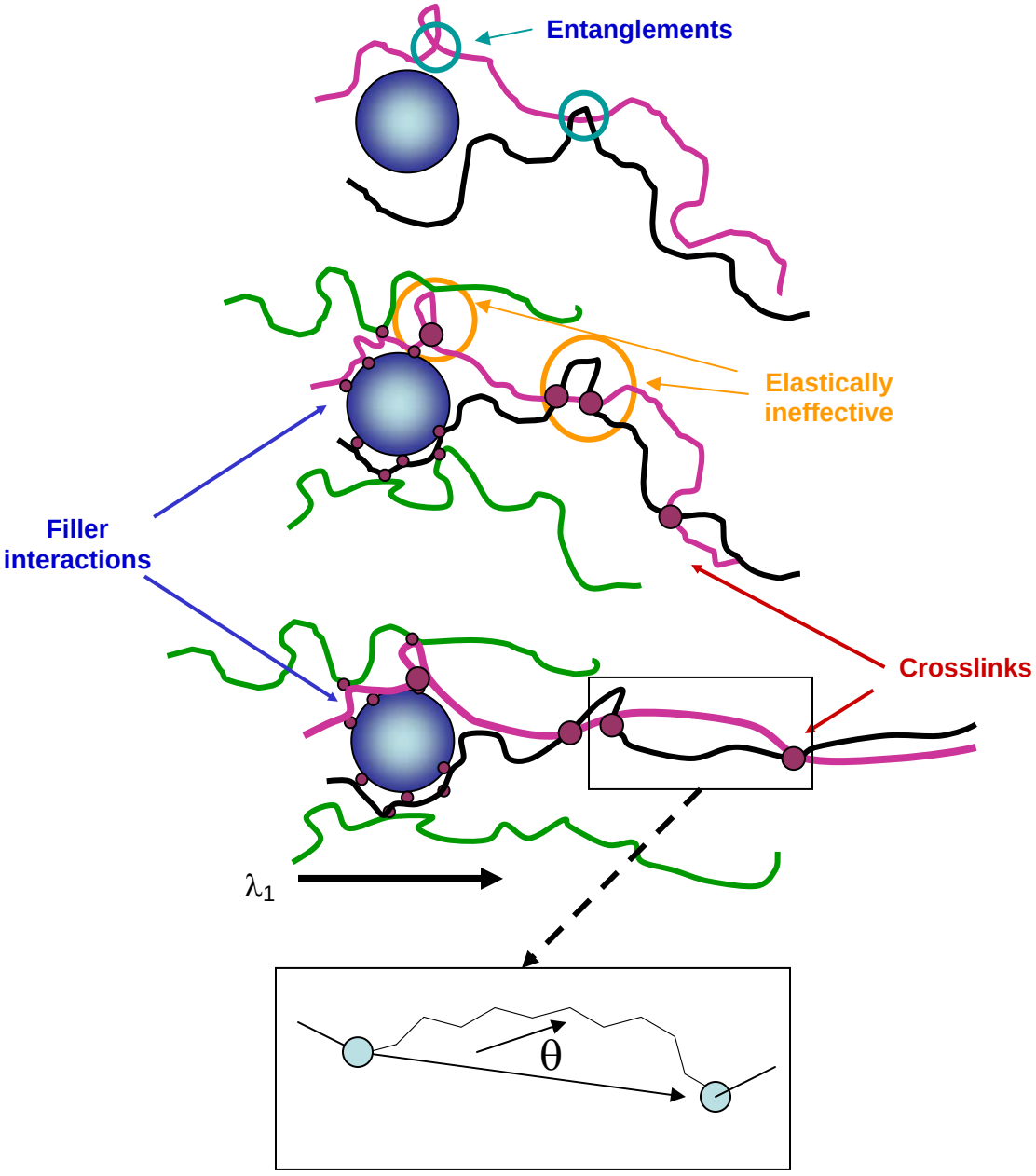
Entanglements
Elastically ineffective
Filler interactions
Crosslinks
λ1
θ